BF2–Azadipyrromethenes: Probing the Excited-State Dynamics of a NIR Fluorophore and Photodynamic Therapy Agent

ARTICLE *in* THE JOURNAL OF PHYSICAL CHEMISTRY A · DECEMBER 2011

Impact Factor: 2.69 · DOI: 10.1021/jp2077775 · Source: PubMed

THE JOURNAL OF PHYSICAL CHEMISTRY A

ARTICLE

pubs.acs.org/JPCA

BF_2-Azadipyrromethenes: Probing the Excited-State Dynamics of a NIR Fluorophore and Photodynamic Therapy Agent

Pinar Batat,[†,‡] Martine Cantuel,[†] Gediminas Jonusauskas,[*,‡] Luca Scarpantonio,[†] Aniello Palma,[§] Donal F. O'Shea,[*,§] and Nathan D. McClenaghan[*,†]

[†]University of Bordeaux/CNRS, Institut des Sciences Moléculaires, 351, crs de la Libération 33405 Talence, France

[‡]University of Bordeaux/CNRS, Laboratoire Ondes et Matières d'Aquitaine, 351, crs de la Libération 33405 Talence, France

[§]School of Chemistry and Chemical Biology, University College Dublin, Belfield, Dublin 4, Ireland

Supporting Information

ABSTRACT: BF_2-Azadipyrromethene dyes are a promising class of NIR emitter (nonhalogenated) and photosensitizer (halogenated). Spectroscopic studies on a benchmark example of each type, including absorption (one and two photon), time-resolved transient absorption (ps−ms) and fluorescence, are reported. Fast photodynamics reveal that intense nanosecond NIR fluorescence is quenched in a brominated analog, giving rise to a persistent (21 μs) transient absorption signature. Kinetics for these changes are determined and ascribed to the efficient population of a triplet state (72%), which can efficiently sensitize singlet oxygen formation (ca. 74%), directly observed by $^1\Delta_g$ luminescence. Photostability measurements reveal extremely high stability, notably for the nonhalogenated variant, which is at least 10^3-times more stable ($\Phi_{photodeg.} = < 10^{-8}$) than some representative BODIPY and fluorescein dyes.

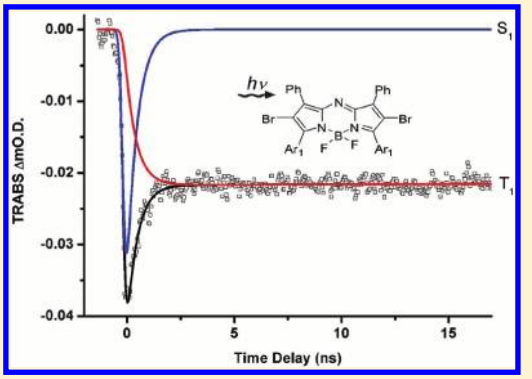

INTRODUCTION

In spite of their useful properties as NIR-emitting fluorophores and singlet oxygen sensitizers, time-resolved studies on BF_2-azadipyrromethene molecules have scarcely been reported. Herein, spectroscopic studies of two analogues (**1** and **2**, Scheme 1), which differ only in the substituent at the β-pyrrole position (H or Br, respectively) are reported. This single structural difference between **1** and **2** has been extensively exploited since its first description in 2002, and at an application level it divides this class of dye into separate categories.[1] Nonhalogenated **1** is suitable for applications harnessing the relatively high fluorescence quantum yields such as fluorochromes,[2] sensors,[3] and donor/acceptor conjugates.[4] Concerning the latter conjugates, one such dye was employed as an electron donor covalently attached to a highly functionalized single-wall carbon nanotube (SWNT) acceptor, with potential for use in organic photovoltaics. In this work, the only study involving subnanosecond optical measurements on this class of dye, femtosecond transient absorption measurements in a small time window showed charge transfer from a photoexcited BF_2-azadipyrromethene donor to the SWNT acceptor, generating a short-lived radical ion pair state with a lifetime of 1.2 ns.[4]

In contrast, the halogenated derivatives **2**, are much less emissive and have been shown to play the role of photosensitizers for singlet oxygen production, a key parameter in PDT. This difference was qualitatively illustrated using comparative measurements of the rate of light-induced oxidative degradation of diphenylisobenzofuran (DPBF) for numerous analogues of **1** and **2**.[1b,5]

These results were consistent with those observed with specific compounds such as **2a** (Ar = Ph and Ar^1 = *p*-$CH_3OC_6H_4$) which have shown in vitro PDT EC50 values in the low nanomolar range with numerous tumor cell types.[6] Studies using a MDA-MB-231 human breast cancer tumor model in mice showed tumor ablation in 71% of animals.[7] A related bis-cationic derivative **2b** (Ar = *p*-Me(Et)$_2N^+CH_2C_6H_4$ and Ar^1 = *p*-$CH_3OC_6H_4$) designed for bacterial uptake and light induced eradication showed excellent results against a broad spectrum of pathogens.[8]

This distinction between nonhalogenated and halogenated derivatives has also been subsequently exploited with dipyrromethene-boron difluoride (BODIPY) chromophores which show many desirable properties and several examples have passed from the academic to the industrial worlds.[9] While nonhalogenated derivatives are widely used for cellular imaging in the 500 to 600 nm range, the halogenated derivatives **4**,[10] **6**,[11] and **8**[12] have recently been investigated for their photodynamic properties. Specifically, **4** has proven excellent in generating reactive oxygen species (ROS) by using the method involving oxidative degradation of DPBF. These results were corroborated with direct quantitative direct singlet oxygen phosphorescence measurements using relative intensities at 1268 nm. In these measurements, **4** was shown to have an ~1.34 times higher efficiency for singlet oxygen generation than methylene blue ($\Phi^1O_2 = 0.79$).[10]

Received: August 13, 2011
Revised: October 17, 2011
Published: October 21, 2011

Scheme 1. β-Pyrrole Halogenated and Non-Halogenated BF_2-Azadipyrromethenes and Dipyrromethenes

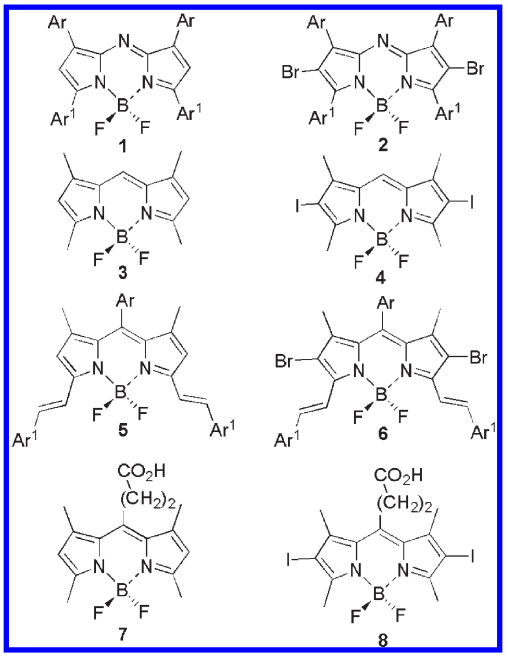

In a comprehensive study of 15 halogenated and nonhalogenated derivatives the di-iodo derivative **8** proved optimal. It gave a 24-fold greater rate of oxidative DPBF trap degradation than methylene blue (Φ^1O_2 = 0.5), with 100-fold better efficacy in vitro when compared to nonhalogenated derivatives and was effective at complete closure of blood vessels with 40 J·cm^{-2} irradiation using the chick embryo CAM model.[12] Recently, a comparative, indirect measurement of the singlet oxygen generation quantum yield of an individual halogenated BF_2-azadipyrromethene was reported at 70%.[13a] The authors later acknowledged the erroneous nature of their hypothesis that this was an improved example over previously reported halogenated derivatives of this class.[13b]

Herein we report a comprehensive study of molecules **1a** and **2a**, utilizing real time measurements in the picosecond to microsecond time domains which has allowed full characterization of absorption and emission properies and processes therein, including quantification of triplet formation and singlet oxygen generation. Additionally, the photodegradation quantum yields for these representative members of halogenated and nonhalogenated BF_2-azadipyrromethene molecules are presented, qualifying them as being viable candidates for applications in NIR fluorescence imaging and PDT.

EXPERIMENTAL SECTION

BF_2-Azadipyrromethenes **1a** and **2a** were synthesized according to previously reported procedures.[1b] Electronic absorption spectra were recorded on a UV−vis-NIR Varian Cary 5000. The transient absorption/time-resolved fluorescence setup was built as follows. A frequency tripled Nd:YAG amplified laser system (30 ps, 30 mJ @1064 nm, 20 Hz, Ekspla model PL 2143) output was used to pump an optical parametric generator (Ekspla model PG 401) producing tunable excitation pulses in the range 410−2300 nm. The residual fundamental laser radiation was focused in a high pressure Xe filled breakdown cell where a white light pulse for sample probing was produced. All light signals were analyzed by a spectrograph (Princeton Instruments Acton model SP2300) coupled with a high dynamic range streak camera (Hamamatsu C7700). Accumulated sequences (sample emission, probe without and with excitation) of pulses were recorded and treated by HPDTA (Hamamatsu) software to produce two-dimensional maps (wavelength vs delay) of transient absorption intensity in the range 300−800 nm. The typical measurement error was better than 10^{-3} OD. Fluorescence emission and excitation spectra of optically dilute solutions were recorded on a Horiba Jobin-Yvon Fluorolog-3 with TCSPC mode, equipped with UV−vis-NIR detector R2658P and NIR detector H10330−45. Absolute quantum yields were determined from fluorescence spectra recorded on the aforementioned spectrofluorometer equipped with a Labsphere optical Spectralon integrating sphere (diameter of 100 mm), which provides a reflectance >99% over 400−1500 nm range (>95% within 250−2500 nm). Solution samples in glass containers were mounted inside the sphere on a Teflon support. Degassed samples were studied in blowtorch sealed cells, having been thoroughly degassed by multiple freeze−pump−thaw cycles. Two Photon Absorption cross sections were measured using an Optical Parametric Generator (OPG) Topas-C (Light Conversion) pumped by a femtosecond laser system Femtopower Compact Pro (Femtolasers) output. The OPG output, after necessary attenuation, was focused with a 50 cm focal length lens. The sample and reference solutions, placed in 1 cm synthetic silica cells, were installed at 30 cm from the lens thereby ensuring a constant beam size in the sample at all wavelengths. The OPG pulse duration in the sample (ca. 40 fs) was fixed for all wavelengths used. Two photon excited fluorescence was observed by a XC-75 (Sony) video camera through an appropriate pump wavelength cutting filter. Carbon tetrachloride, which is transparent to at least 1600 nm, was used to dissolve samples.

RESULTS AND DISCUSSION

Electronic Absorption and Fluorescence Emission Spectra of BF_2-Azadipyrromethene Dyes 1a and 2a. Steady-state electronic absorption and fluorescence spectra of **1a** and **2a** have been previously reported in various solvents, with absorption maxima at 682 and 665 nm and emission maxima in CH_3CN at 721 and 716 nm, respectively (see SI), thus showing an increased Stokes' shift in the case of **2a** compared to **1a**, 1072 cm^{-1} cf. 793 cm^{-1}.[1b] Significantly different fluorescence quantum yields between **1a** and **2a** were previously established in optically dilute solution, 0.36 *cf.* 0.1, respectively.[1b] Absolute quantum yield values in acetonitrile were obtained through photon counting measurements on a fluorimeter equipped with an integrating sphere (see SI for details), showing excellent agreement with the values previously determined in chloroform, and giving quantum yield values of 0.35 and 0.10, respectively. Considering NIR-emitting **1a**, the monoexponential fluorescence decay gave a measured fluorescence lifetime (τ_0) of 2.2 ns (see SI for decay). Applying eq 1 allows determination of the radiative rate constant, which was determined to be 1.6 × 10^8 s^{-1}, a value for k_r of similar magnitude to those observed for BODIPY chromophores.[9]

$$k_r = \frac{\Phi_f}{\tau_0} \quad (1)$$

$$\frac{1}{\tau_{rad}} = 2.88 \times 10^{-9} n^2 \langle \nu_F^{-3} \rangle^{-1} \int \frac{\varepsilon(\nu)}{\nu} d\nu \quad (2)$$

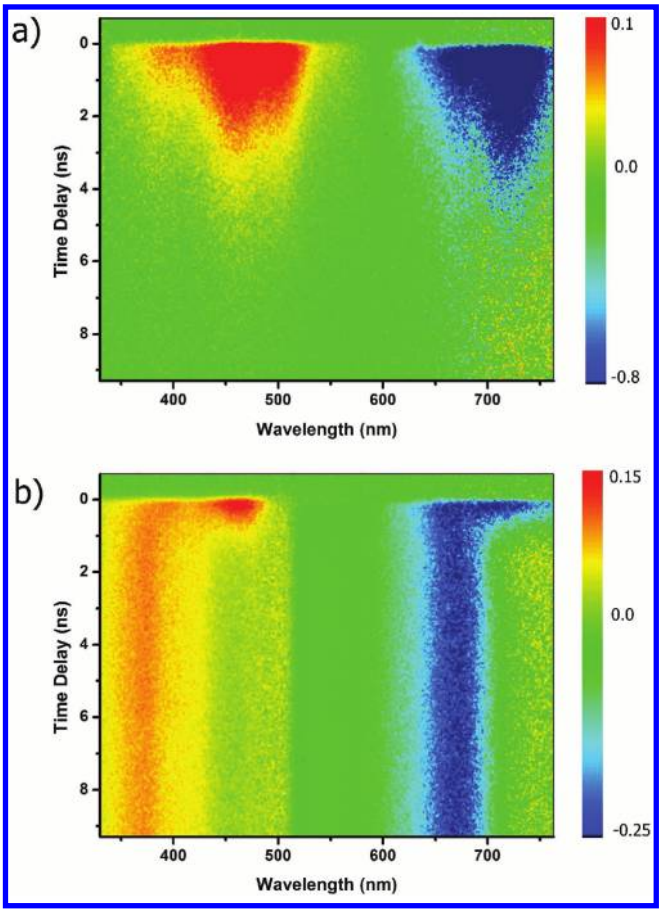

Figure 1. Transient absorption spectra with different time delays following excitation in CH_3CN: (a) **1a**; (b) **2a**. (See SI and Figure 2 for kinetics). Each spectrum is constructed from two spectra: excitation 650 and 460 nm.

Applying a Strickler–Berg treatment (eq 2), where n is the refractive index of the solvent (assumed to be the same in all spectral regions), ε is the molar absorptivity, and $<\nu_f^{-3}>$ is the reciprocal of the mean value of ν^{-3} across the fluorescence spectrum, allows estimation of the natural lifetime (τ_{rad}).[14] Substituting the reciprocal of the natural lifetime (k_r) into eq 1 gives an estimated fluorescence lifetime of 2.8 ns for **1a**, which is in good agreement with the measured value of 2.2 ns. This suggests that the excited state of **1a** is structurally reminiscent to that of the ground-state and that only a small structural reorganization takes place and that solvent interactions are unchanging.

The lowered quantum yield for **2a** suggests the presence of a supplementary/enhanced deexcitation pathway in this case. Additionally, the measured fluorescence lifetime is significantly shorter in the case of **2a** compared to **1a**, 550 ps versus 2.2 ns. This lifetime change closely mirrors the quantum yield change and no evidence for supplementary emission is observed. (Note: a prompt anisotropic emission component ca. 80 ps is observed in both cases, which gives a measure of molecular rotation rate and solvent reorganization, see SI). The most straightforward explanation for the difference in total fluorescence emission and fluorescence lifetime between **1a** and **2a** is enhanced intersystem crossing and population of a low-lying triplet state in the case of **2a** due to the presence of two heavy bromine atoms, replacing the β-protons of **1a**. The population of the triplet state has been

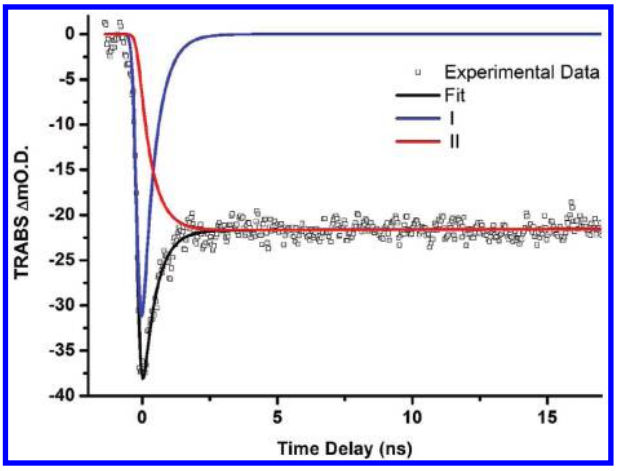

Figure 2. Evolution of transient absorption signal (TRABS) at 660 nm of **2a** at different time delays in degassed CH_3CN (λ_{exc} = 635 nm). Blue trace (I) shows singlet state decaying and the red trace (II) shows triplet state grow-in.

observed for some analogous BODIPY chromophores bearing heavy transition metal ions[15] and is a prerequisite for the observed efficient photosensitization of molecular oxygen with **2a**, previously reported in singlet oxygen trapping experiments with DPBF. Assuming the inherent radiative rate constant remains comparable to structurally similar **1a**, the rate of intersystem crossing (k_{ISC}) in **2a** could be estimated using eq 3, where τ_f is the lifetime of the quenched fluorescence and $1/\tau_0$ is the rate of the unquenched fluorescence, giving an intersystem crossing rate of 1.4×10^9 s^{-1} in **2a**.

$$k_{ISC} = \frac{1}{\tau_f} - \frac{1}{\tau_0} \quad (3)$$

Transient Absorption Spectroscopic Studies of BF_2-Azadipyrromethene Dyes 1a and 2a. To check the validity of the aforementioned intersystem crossing value, to directly visualize the triplet grow-in and to evaluate the efficiency of intersystem crossing, complementary transient absorption spectroscopy was performed. Significantly different transient absorption spectra were recorded for **1a** (Figure 1a) and **2a** (Figure 1b) following excitation of the lowest energy absorption band (see SI for slices and excited singlet and triplet absorption spectra). In addition to a ground-state bleaching band, specific positive signatures are observed, notably that at 460 nm, which decays at a similar rate to the fluorescence and thus deexcitation of the S_1 state, allowing attribution to an $S_n \leftarrow S_1$ transition. Meanwhile, excited **2a** shows a similar absorption band, whose rapid decay is concomitant with the grow-in of a different persistent band whose absorption lies at 370 nm, attributed to triplet absorption ($T_n \leftarrow T_1$) with singlet-to-triplet intersystem crossing occurring at a rate of 1.5×10^9 s^{-1}; thus being extremely similar to the value obtained from fluorescence changes. The correlated kinetics for concomitant singlet decay and triplet grow-in are shown in Figure 2. Additionally, the quantum yield of intersystem crossing can be directly determined based on prompt changes in the absorption band corresponding to ground-state bleaching, on going from the initial photogenerated value to the metastable triplet population after a few nanoseconds, which is readily measured off Figure 2. Thus an intersystem crossing quantum efficiency of 0.72 in **2a**

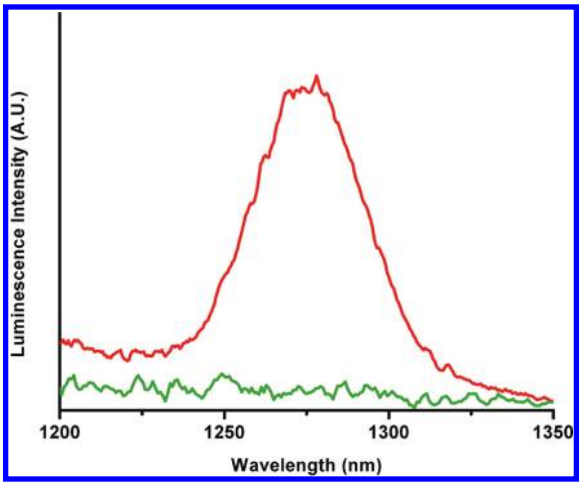

Figure 3. Phosphorescence of $^1O_2$ sensitized by isosbestic solutions of **1a** (green) and **2a** (red) in air-equilibrated CH_3CN (Note: residual fluorescence of **1a** and **2a** in degassed solutions has been subtracted).

was determined. This high value is well-suited for applications in photodynamic therapy, and shows intersystem crossing to be the major loss difference between **1a** and **2a**.

The lifetime of this newly formed absorption band was recorded at different concentrations in deaerated solution in order to eliminate potential contributions from self-quenching. Extrapolating a plot of $1/\tau$ vs concentration to infinite dilution allowed estimation of the unquenched triplet lifetime to be 21 μs (see SI). At comparable concentrations, similar room temperature triplet lifetimes were reported for a ruthenium-BODIPY dyad and triad (8 and 30 μs, respectively).[15]

Singlet Oxygen Sensitization. Important considerations for photosensitizer dyes, particularly with respect to singlet oxygen generation, are that the triplet state of the photosensitizer is sufficiently long-lived to participate in a diffusion-limited bimolecular reaction with dissolved oxygen (typically via dynamic excited-state quenching due to electronic energy transfer) and is of appropriate energy ($\geq$0.98 eV). Triplet state energies can be conveniently derived from phosphorescence spectra, however no phosphorescence was observed from **1a** or **2a** in low temperature glasses (77 K butyronitrile) even in the presence of external heavy atoms (ethyl iodide/solvent, up to 10%, v/v). A similar outcome has been reported for BODIPY derivatives which required incorporation of transition metals to allow direct observation of phosphorescence in only a few isolated cases.[15]

Reported ab initio calculations, which are typically challenging for excited species, afforded an estimation of the singlet−triplet gap in **2a** to be 0.90 eV, which when considering the experimentally measured singlet energy of 1.81 eV, would make the triplet rather low in energy at ca. 0.91 eV, to efficiently sensitize triplet oxygen.[16]

Previously, generation of singlet oxygen using BF_2-azadipyrromethene dyes was deduced from indirect methods by use of chemical trapping agents such as DPBF, which are more suited to qualitative descriptions. Observation of singlet oxygen phosphorescence would therefore allow an alternative, direct evaluation of the role of these molecules in singlet oxygen sensitization. Figure 3 shows the phosphorescence of singlet oxygen (λ_{max} = 1270 nm) obtained on exciting air-equilibated isosbestic solutions of **1a** and **2b** in acetonitrile at room temperature. With little evidence of intersystem crossing from transient absorption measurements, excited **1a** does not generate singlet oxygen, while the relatively high, long-lived triplet population of **2a** is several orders of magnitude more efficient in this regard. This marked difference between **1a** and **2a** sensitization capacities are in agreement with our previous indirect DPBF trapping experiments in vitro and in vivo efficacy studies.[1b,7]

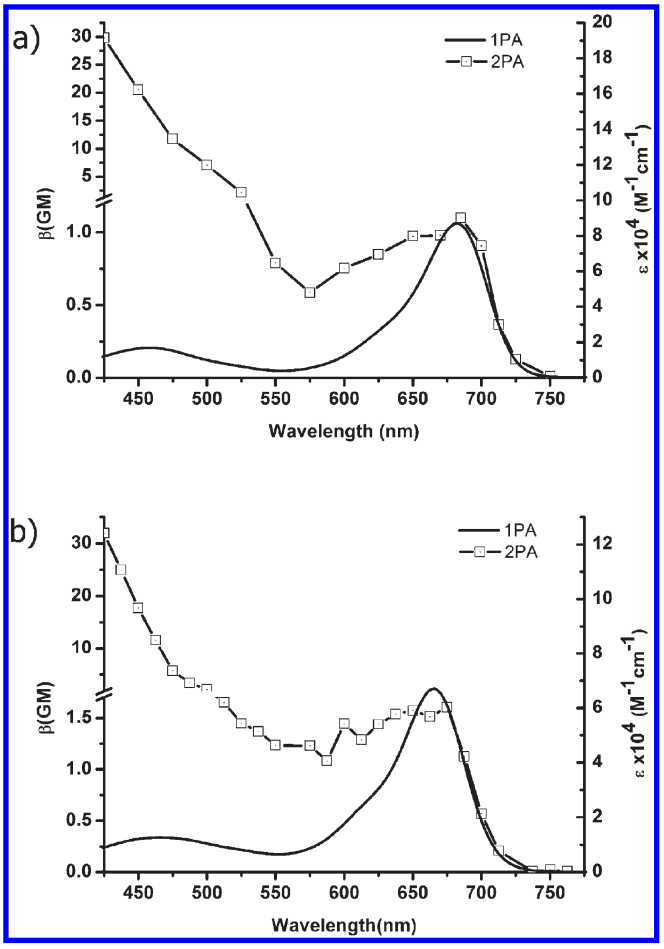

Figure 4. Comparative one and two-photon absorption spectra of solutions of (a) **1a** and (b) **2a**.

Singlet oxygen emission is strongly dependent on solvent parameters due to the close-lying dark $^1\Sigma_g^+$ and emissive $^1\Delta_g$ states such that even small variations in solvation have dramatic effects of oxygen emission, as well as differences arising from solvent-specific oxygen concentrations and diffusion rates.[17] Thus the singlet oxygen generation capacity was compared to C_{60}, a popular standard in the same solvent (toluene). The singlet oxygen producing efficiency of fullerene was established to be 0.96 on visible excitation.[18] The relative integrated singlet oxygen emission intensity obtained with **2a** was ca. 0.77 that obtained with C_{60}, giving an absolute $^1O_2$-generation value of 74%. This value, which is within experimental error of the measured triplet quantum yield, highlights the efficient bimolecular sensitizer-to-oxygen energy transfer reaction.

Two Photon Absorption Spectroscopy. To further investigate some fundamental spectroscopic properties of **1a** and **2a**, and notably to verify potential differences due to the inclusion of heavy bromine atoms, the two-photon absorption spectra were obtained for these representative molecules. Figure 4 shows comparative one and two-photon absorption (denoted 1PA and 2PA, respectively) spectra for **1a** (Figure 4a) and **2a** (Figure 4b),

dx.doi.org/10.1021/jp2077775 |J. Phys. Chem. A 2011, 115, 14034–14039

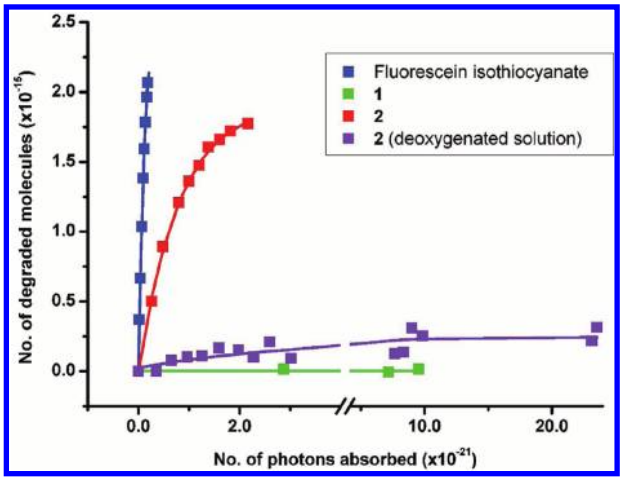

Figure 5. Advancement of photodegradation of **1a** and **2a** compared to fluorescein on exciting dilute solutions (**1a** and **2a**: λ_{exc} = 640 nm in acetonitrile; fluorescein isothiocyanate: λ_{exc} = 504 nm in ethanol, respectively). Solutions are air-equilibrated unless otherwise stated.

with the two-photon absorption spectra having been obtained by 2PA-induced fluorescence measurements. The molecular two photon cross section (β, quoted in the units of Goeppert-Mayer) was determined according to eq 4, where F represents the fluorescence intensity, W is the pump power, φ is the quantum yield of fluorescence, C is the concentration. Rhodamine 6G (590) dye two photon absorption was used as a reference (β = 9.5 GM at 1050 nm).[19]

$$\beta(\lambda) = \frac{F(\lambda)W_{1050}^2}{F_{1050}^{Rh6G}W^2(\lambda)}\left(\frac{1050}{\lambda}\right)^2\frac{\varphi^{Rh6G}C^{Rh6G}}{\varphi^{sample}C^{sample}}\beta_{1050}^{Rh6G} \quad (4)$$

Generally, as noted previously, in the absence of additional push−pull chromophores, the NIR two photon absorption cross section of BF_2-azadipyrromethenes is modest,[20] although it is worth highlighting that in spite of relatively small TPA cross sections, hydrosoluble conventional BODIPY dyes were successfully used in two-photon imaging microscopy.[21] However, it is instructive to observe the TPA behavior in the visible spectral region and make a comparison between **1a** and **2a**. Each TPA spectrum (Figure 4) matches the wavelength doubled linear one, as typically observed for noncentrosymmetric compounds, indicating that the same transition is one- and two-photon allowed.[22] The response of **2a** is slightly higher for the lowest energy band compared to **1a**, while the molar absorptivity for one photon absorption is significantly less and broader (fwhm = 1430 cm^{-1} cf. 1250 cm^{-1}).

Lowered 1PA and increased 2PA in brominated **2a** compared to nonbrominated **1a** suggests some bromine-induced perturbations although structural difference or changes in the calculated natural lifetime is not significant as denoted by time-resolved fluorescence (vide supra), making the major difference between **1a** and **2a** the heavy atom-induced intersystem crossing pathway.

Photostability Measurements of BF_2-Azadipyrromethene Dyes 1a and 2a. The photostability of dyes is an important parameter for different applications, including imaging. Indeed, limited photostability can prove a major limitation to implementation in demanding laser experiments, for example, single molecule spectroscopy experiments, making development of highly photostable species an active research area.[23] In an effort to quantify the photostability of halogenated and nonhalogenated dyes, the absorption changes as a function of irradiation time was measured for **1a** and **2a**, along with that of fluorescein isothiocyanate and 4-iodophenyl-BODIPY, for comparison. The quantum yield for photodegradation could thus be determined (see SI for detailed description). Subsequently, this can be converted to the number of photodegraded molecules as a function of number of photons absorbed, which allows visualization of the relative stability of the molecules. Figure 5 shows the relative stabilities of **1a**, **2a** and fluorescein isothiocyanate in air-equilibrated solution, as well as **2a** in deoxygenated solution.

Fluorescein isothiocyanate, although a widely used label in microscopy experiments and fluorescence imaging, can be seen to be the least stable species, followed by the brominated **2a** in the presence of oxygen. Most noteworthy is the extreme photostability of molecule **1a**, which proved so photostable that the value cannot be accurately determined in acetonitrile solvent. Indeed, no discernible change could be observed even after several days of continuous laser irradiation in air-equilibrated solution. Quantum yield values (Φ_{deg}) of 7.5 × 10^{-5} for fluorescein isothiocyanate in ethanol was measured, in good agreement with a literature value (in deaerated ethanol); Φ_{deg} = 1.8 × 10^{-5} was measured for the 4-iodo-BODIPY, while a value of 2.7 × 10^{-5} for a pentafluorophenylBODIPY was recently reported.[24,25] Significantly lower values (and thus higher stability) for BF_2-azadipyrromethene dyes **1a** (<10^{-8}) and **2a** (5.4 × 10^{-8}) were determined in air-equilibrated and deoxygenated acetonitrile, respectively. Dye **2a** shows some additional degradation on short time scales in air-equilibrated solution, which is attributed to singlet oxygen attack on the photosensitizer on comparing with the deoxygenated case in Figure 5, as well as direct photodamage. Concerning **1a**, a value of 9.6 × 10^{-8} was determined in DMSO solvent (see SI for photodegradation curve in acetonitrile compared with DMSO). Such an extremely low degradation value, which is around 3-orders of magnitude lower than fluorescein or BODIPY derivatives, even in the absence of any precautions such as degassing or incorporation into a polymer matrix, is promising for challenging imaging applications.

CONCLUSIONS

Dibrominated BF_2-azadipyrromethene **2a** has proven to be an effective sensitizer for the generation of singlet oxygen, evidenced directly through singlet oxygen emission, with an estimated quantum yield of 74%, or 0.77 compared to C_{60}. Importantly, evolution of the singlet ($S_n \leftarrow S_1$) and triplet ($T_n \leftarrow T_1$) transient absorption signatures of different members of this class of molecule allows direct spectroscopic determination of the rate and efficiency of intersystem crossing to the nonemissive triplet state of **2a** and lifetime of this PDT-active excited state. An intersystem crossing efficiency of 72% was determined with a triplet lifetime of 21 μs, making halogenated BF_2-azadipyrromethenes therapeutically interesting red-light absorbing photosensitizers. Collectively taking the results presented here for **1a** and **2a** along with those previously reported for compounds **4**, **6**, and **8** it can be concluded that heavy-atom substitution, notably with Br or I, at the β-pyrrole position has a general consequence of enhancing triplet state population. Ongoing work into the excited-state properties of **1a**, **2a** and related compounds will be reported in due course. Additionally, we have shown the exceptional photostability of these dyes, notably in the case of the

nonhalogenated BF_2-azadipyrromethene, whose photodegradation quantum yield is at least 1000-times lower than fluorescein isothiocyanate or selected BODIPY molecules. Current related work concerns studies on other analogues and integration into supramolecular and biological systems.

■ ASSOCIATED CONTENT

Supporting Information. Steady-state electronic absorption, fluorescence excitation, and emission spectra. Fluorescence and fluorescence anisotropy decays, absolute quantum yield determination, transient absorption spectra, excited singlet and triplet absorption spectra, concentration dependent triplet lifetime, determination of photodegradation quantum yields. This information is available free of charge via the Internet at http://pubs.acs.org.

■ AUTHOR INFORMATION

Corresponding Author

*E-mail: g.jonusauskas@loma.u-bordeaux1.fr (G.J.);donal.f.oshea@ucd.ie(D.F.O); n.mc-clenaghan@ism.u-bordeaux1.fr; Fax: (+33) 5 40 006158 (N.D.M.).

■ ACKNOWLEDGMENT

Financial support from the European Research Council under the European Community's Seventh Framework Programme (FP7/2008-2013) ERC Grant Agreement No. [208702]; Région Aquitaine; CNRS (M.C.), Ministère de la Recherche et de l'Enseignement Supérieur (P.B) and Science Foundation Ireland (A.P.) is gratefully acknowledged.

■ REFERENCES

(1) (a) Killoran, J.; Allen, L.; Gallagher, J. F.; Gallagher, W. M.; O'Shea, D. F. *Chem. Commun.* **2002**, 1862–1863. (b) Gorman, A.; Killoran, J.; O'Shea, C.; Kenna, T.; Gallagher, W. M.; O'Shea, D. F. *J. Am. Chem. Soc.* **2004**, *126*, 10619–10631.

(2) (a) Tasior, M.; O'Shea, D. F. *Bioconjugate Chem.* **2010**, *21*, 1130–1133. (b) Murtagh, J.; Frimannsson, D. O.; O'Shea, D. F. *Org. Lett.* **2009**, *11*, 5386–5389.

(3) Palma, A.; Tasior, M.; Frimannsson, D. O.; Vu, T. T.; Meallet-Renault, R.; O'Shea, D. F. *Org. Lett.* **2009**, *11*, 3638–3641. (b) Hall, M. J.; Allen, L. T.; O'Shea, D. F. *Org. Biomol. Chem.* **2006**, *4*, 776–780. (c) Gawley, R. E.; Mao, H.; Mahbubul Haque, M.; Thorne, J. B.; Pharr, J. S. *J. Org. Chem.* **2007**, *72*, 2187–2191. (d) Loudet, A.; Bandichhor, R.; Wu, L.; Burgess, K. *Tetrahedron* **2008**, *64*, 3642–3654.

(4) Flavin, K.; Lawrence, K.; Bartelmess, J.; Tasior, M.; Navio, C.; Bittencourt, C.; O'Shea, D. F.; Guldi, D. M.; Giordani, S. *ACS Nano* **2011**, *5*, 1198–1206.

(5) McDonnell, S. O.; Hall, M. J.; Allen, L. T.; Byrne, A.; Gallagher, W. M.; O'Shea, D. F. *J. Am. Chem. Soc.* **2005**, *127*, 16360–16361.

(6) Gallagher, W. M.; Allen, L. T.; O'Shea, C.; Kenna, T.; Hall, M.; Gorman, A.; Killoran, J.; O'Shea, D. F. *Br. J. Cancer* **2005**, *92*, 1702–1710.

(7) (a) Byrne, A. T.; O' Connor, A.; Hall, M.; Murtagh, J.; O' Neill, K.; Curran, K. M.; Mongrain, K.; Rousseau, J. A.; Lecomte, R.; McGee, S.; et al. *Br. J. Cancer* **2009**, *101*, 1565–1573. (b) O'Connor, A. E.; McGee, M. M, Likar, Y.; Ponomarev, V.; Callanan, J. J.; O'Shea, D. F.; Byrne, A. T.; Gallagher, W. M. *Intern. J. Cancer* 2011, DOI: 10.1002/ijc.26073.

(8) Frimannsson, D. O.; Grossi, M.; Murtagh, J.; Paradisi, F.; O'Shea, D. F. *J. Med. Chem.* **2010**, *53*, 7337–7343.

(9) (a) Loudet, A.; Burgess, K. *Chem. Rev.* **2007**, *107*, 4891–4932. (b) Benniston, A. C.; Copley, G. *Phys. Chem. Chem. Phys.* **2009**, *11*, 4124–4131. (c) Ziessel, R.; Ulrich, G.; Harriman, A. *New. J. Chem.* **2007**, *31*, 496–501.

(10) Yogo, T.; Urano, Y.; Ishitsuka, Y.; Maniwa, F.; Nagano, T. *J. Am. Chem. Soc.* **2005**, *127*, 12162–12163.

(11) Ozlem, S.; Akkaya, E. U. *J. Am. Chem. Soc.* **2009**, *131*, 48–49.

(12) Lim, S. H.; Thivierge, C.; Nowak-Sliwinska, P.; Han, J.; van den Bergh, H.; Wagnières, G.; Burgess, K.; Lee, H. B. *J. Med. Chem.* **2010**, *53*, 2865–2874.

(13) (a) Adarsh, N.; Avirah, R. R.; Ramaiah, D. *Org. Lett.* **2010**, *12*, 5720–5723. (b) Adarsh, N.; Avirah, R. R.; Ramaiah, D. *Org. Lett.* **2011**, *13*, 2146–2146.

(14) (a) Strickler, S. J.; Birks, R. A. *J. Chem. Phys.* **1962**, *37*, 814–822. (b) Birks, J. B. *Photophysics of Aromatic Molecules*; Wiley Interscience: London, 1970.

(15) (a) Galletta, M.; Campagna, S.; Quesada, M.; Ulrich, G.; Ziessel, R. *Chem. Commun.* **2005**, 4222–4224. (b) Nastasi, F.; Puntoriero, F.; Campagna, S.; Diring, S. *Phys. Chem. Chem. Phys.* **2008**, *10*, 3982–3986.

(16) (a) Quartarolo, A. D.; Russo, N.; Sicilia, E. *Chem.—Eur. J.* **2006**, *12*, 6797–6803. (b) Fabian, J. *Dyes Pigm.* **2009**, *84*, 36–53.

(17) Due to solvent-dependent radiative rate constants for singlet oxygen phosphorescence, as well as oxygen concentration and diffusion coefficients, the same solvent was used in estimating φ. (a) Gorman, A. A.; Krasnovskii, A. A.; Rodgers, M. A. J. *J. Phys. Chem.* **1991**, *95*, 598–601. (b) Wilkinson, F.; Helman, W. P.; Ross, A. B. *J. Phys. Chem. Ref. Data* **1995**, *24*, 663–677. (c) Schweitzer, C.; Schmidt, R. *Chem. Rev.* **2003**, *103*, 1685–1757.

(18) Arbogast, J. W.; Darmanyan, A. P.; Foote, C. S.; Rubin, Y.; Diederich, F. N.; Alvarez, M. M.; Anz, S. J.; Whetten, R. L. *J. Phys. Chem.* **1991**, *93*, 11–12.

(19) Makarov, N. S.; Drobizhev, M.; Rebane, A. *Opt. Express* **2008**, *16*, 4029–4047.

(20) Bouit, P.-A.; Kamada, K.; Feneyrou, P.; Berginc, G.; Toupet, L.; Maury, O.; Andraud, C. *Adv. Mater.* **2009**, *21*, 1151–1154.

(21) (a) Nicolini, C.; Baranski, J.; Schlummer, S.; Palomo, J.; Lumbierres-Burgues, M.; Kahms, M.; Kuhlmann, J.; Sanchez, S.; Gratton, E.; et al. *J. Am. Chem. Soc.* **2006**, *128*, 192–201. (b) Bestvater, F.; Spiess, E.; Strobrawa, G.; Hacker, M.; Feurer, T.; Porwol, T.; Berchner-Pfannschmidt, U.; Wostlaw, C.; Acker, H. *J. Microsc.* **2002**, *208*, 108–115.

(22) (a) Boyd, R. W. *Non-Linear Optics*, 3rd ed.; Academic Press: San Diego, 2008.; (b) He, G. S.; Tan, L.-S.; Zheng, Q.; Prasad, P. N. *Chem. Rev.* **2008**, *108*, 1245–1330.

(23) (a) Fernandez-Suarez, M.; Ting, A. Y. *Nat. Rev. Mol. Cell Biol.* **2008**, *9*, 929–943. (b) Dyba, M.; Hell, S. W. *Appl. Opt.* **2008**, *42*, 5123–5129. (c) Davies, M.; Jung, C.; Wallis, P.; Schnitzler, T.; Li, C.; Müllen, K.; Brauchle, C. *ChemPhysChem* **2011**, *12*, 1588–1595.

(24) Meallier, P.; Guittonneau, S.; Emmelin, C.; Konstantinova, T. *Dyes Pigm.* **1999**, *40*, 95–98.

(25) Vives, G.; Giansante, C.; Bofinger, R.; Raffy, G.; Del Guerzo, A.; Kauffmann, B.; Batat, P.; Jonusauskas, G.; McClenaghan, N. D. *Chem. Commun* **2011**, *47*, 10425–10427.